

ARTICLE

<https://doi.org/10.1038/s41467-019-09475-5>

OPEN

The negative emission potential of alkaline materials

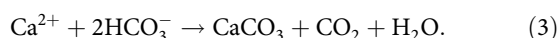
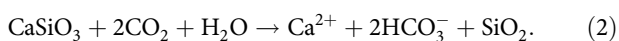
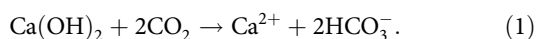
Phil Renforth¹

7 billion tonnes of alkaline materials are produced globally each year as a product or by-product of industrial activity. The aqueous dissolution of these materials creates high pH solutions that dissolve CO₂ to store carbon in the form of solid carbonate minerals or dissolved bicarbonate ions. Here we show that these materials have a carbon dioxide storage potential of 2.9–8.5 billion tonnes per year by 2100, and may contribute a substantial proportion of the negative emissions required to limit global temperature change to <2 °C.

¹School of Engineering and Physical Sciences, Heriot-Watt University, Edinburgh EH14 4AS, UK. Correspondence and requests for materials should be addressed to P.R. (email: P.Renforth@hw.ac.uk)

In addition to substantial cuts in greenhouse gas emissions, humanity may need to remove a large amount of carbon dioxide from the atmosphere to avoid climate change. The ability to remove multiple Gt of CO₂ every year is an important feature of integrated assessment models and particularly those that result in global mean surface temperature increases less than 2 °C^{1–3}. By 2100, this cumulative negative emission requirement may be on the order of 100 to 1000 GtCO₂ (~1 to 15 GtCO₂ yr⁻¹) in 1.5 °C pathways with little or no overshoot and is mostly met by biomass energy carbon capture and storage and afforestation³. There is uncertainty in the potential of most negative emission technologies, which may constrain the rate and extent of their scale-up^{4,5}. Technologies that propose to remove CO₂ from the atmosphere by chemical reaction with natural or artificial minerals are included in literature assessments of negative emissions, but have received substantially less attention compared to other proposals⁶.

Here we consider the potential of negative emissions within existing global industries. Particularly by weathering materials produced from the manufacturing of steel, aluminium, cement, lime, nickel, and from the combustion of coal or biomass. The alkaline materials produced from these activities include blast furnace and steel slag, red mud, cement kiln dust, concrete in building products and demolition waste, ultramafic waste rock and mine tailings and fuel ashes/residue. These materials contain silicate and hydroxide minerals that can dissolve in water and react with CO₂ to produce aqueous bicarbonate ions. If these bicarbonate ions were conveyed to the ocean (e.g., in river water), they would contribute to ocean alkalinity, potentially ameliorating some of the impacts of ocean acidification, and remain in solution for >100,000 years⁷. This enhanced weathering process^{7,8} (Eqs. (1) and (2)) requires that the bicarbonate ions are stored in the ocean, otherwise additional mineral dissolution would lead to the formation of solid carbonate minerals in which some of the CO₂ may be trapped for millions of years (known as mineral carbonation, e.g.⁹, Eqs. (1 + 3) and Eqs. (2 + 3)).



While both mechanisms result in carbon dioxide sequestration, almost twice as much CO₂ is removed through enhanced weathering compared to mineral carbonation (the ratio is closer 1.5–1.8⁷), which is highly desirable when material supply is limited. However, there is little research that examines the environmental consequences of increasing ocean alkalinity, and particularly the impact of harmful trace elements that are present in some alkaline materials⁷. While the residence time of bicarbonate ions in the ocean is effectively permanent, this may be reduced if alkalinity is elevated⁷. As such, storage of carbon dioxide as a mineral carbonate may be the preferred mechanism, which would also reduce the potential for environmental harm^{10,11}. Both mechanisms have been included in this assessment of storage potential.

Carbon dioxide sequestration has been demonstrated using these materials in elevated temperature and high CO₂ pressure (HTP) reactor experiments^{12,13}. However, there is also evidence that atmospheric CO₂ is sequestered under ambient conditions^{14–16}. These materials are created by emission intensive industries, and it is therefore reasonable to suggest that the carbon sequestration potential of the by-products should be used to offset some of these emissions. For instance, the steel industry creates approximately 2200 kg CO₂ t⁻¹ of steel, which equates to around 12,000 kg CO₂ t⁻¹ of by-product slag

(Table 1, column a and Supplementary Notes 1, 2, and 3). The Intergovernmental Panel on Climate Change (IPCC)³ considers that extensive mitigation (e.g., decarbonised energy, carbon capture and storage, energy efficiency improvements) may be able to reduce the emissions intensity to 200–500 kg CO₂ t⁻¹ of steel (or ~1000 kg CO₂ t⁻¹ slag, column b). Some postulate that the integration of hydrogen into steel making may reduce emissions to <60 kg CO₂ t⁻¹ (<300 kg CO₂ t⁻¹ slag)¹⁷. The carbon dioxide capture potential through mineral carbonation or enhanced weathering of slag is 368–620 kg CO₂ t⁻¹. Therefore, only a small proportion of current emissions from most of these industries can be offset by the carbon sequestration in alkaline wastes/by-products. However, by pursuing extensive mitigation together with atmospheric carbon dioxide sequestration in alkaline materials, it may be possible to create industries with net negative emissions, and thus contribute to limiting temperature change to <2 °C.

Here we examine the potential of alkaline materials to remove CO₂ from the atmosphere by forecasting production to 2100, and show that a large proportion of the future negative emission requirements may be met through weathering or carbonation of these materials.

Results

The potential of alkaline material streams. Manufacturing iron and steel produces a range of alkaline wastes/by-products that are rich in oxide, hydroxide and silicate minerals and glasses, collectively referred to as slag. The physical and chemical properties, and the environmental behaviour, of slag depends on the raw materials, the process of creating iron and steel and the method of disposal. Blast furnace slag is commonly used as secondary aggregate, pozzolan or agricultural lime^{18–20}. However, due to the higher concentrations of oxides and hydroxides, slags from steel production are typically stockpiled²¹. These sites have highly alkaline leachates with pH > 10²¹ and can pose environmental issues via extreme pH and potential metal pollution²². CO₂ uptake buffers the waters back towards circum-neutral pH, which also limits metal solubility. HTP mineral carbonation experiments have shown 50–75% conversion of slag over 30 min¹². However, studies investigating legacy deposits have demonstrated CO₂ uptake and carbonate precipitation within the drainage waters and surrounding environments²¹.

Cement is produced by heating limestone (CaCO₃) in a kiln with a source of silicon (clay/shale) to produce metastable calcium silicate minerals (clinker, e.g., Ca₂SiO₄). The clinker is hydrated during construction to produce mortar and concrete. These materials, together with by-product cement kiln dust, have been successfully carbonated in HTP experiments^{11,13}, during curing under elevated CO₂ concentrations²³, during the life of the structure²⁴, when mixed into urban soils following demolition¹⁴, or within leachate management systems of landfill²⁵.

Like cement, lime is produced by heating limestone in a kiln but is subsequently used in numerous industries (Supplementary Note 4 and Supplementary Table 1²⁶). Of the lime produced in the United States and European Union, 30–40% is used by the steel industry as a fluxing agent, 14% is used in other industries (sugar refining, glass, paper, precipitated calcium carbonate), 10–20% is used in construction and 16–24% is used for environmental remediation/treatment (flue gas desulphurisation, water treatment, acid mine drainage). Approximately 20% of lime is used in activities that exploit reactions with CO₂ (e.g., regenerating NaOH in the Kraft process) or weathering (e.g., agricultural liming). Approximately 14% of the lime is used in activities that do not have an explicit reaction with CO₂, but it may be possible to engineer this within the life cycle of the material (e.g., soda lime glass, soil stabilisation).

Table 1 Carbon production intensities and sequestration potential of highly alkaline materials, by-products and wastes

Material	2010 CO ₂ intensity ^a	2050 CO ₂ intensity ^b	Carbonation potential ^c	Measured carbonation ^d	Enhanced weathering potential ^e	Carbon offset recycling/reuse ^f
Blast furnace slag			413 ± 13	90–230	620 ± 19	
Basic oxygen furnace slag	12,000	2700–4300	402 ± 17		602 ± 25	-100. Up to 700 in high substitution specialised cements.
Electric arc furnace slag		(286–1080) ⁱ	368 ± 10	50–540	552 ± 15	<5 as aggregate
Ordinary portland cement	800	200–400	510	300	773	—
		(100–200) ^j				
Cement kiln dust	6900 ^g	1700–3500	330 ± 12	82–260	530 ± 21	-0 Recycled into kiln
Construction and demolition waste	—	—	77–110	—	110–190	<5 As aggregate
Lime	1000	200 ^h	777 ± 13	—	1165 ± 19	—
Ultraplastic mine tailings	8–250	—	40–250	<50	60–377	—
Hard coal ash			36 ± 6	20–30	73 ± 10	
Lignite ash	20,000	(2000–2600) ^j	146 ± 28	230–264	246 ± 52	
Marine algae biomass ash			31	—	348	
Wood/woody biomass ash			–89–815		–118 to 1766	
Herbaceous and agricultural biomass ash	490	<–16,200	–239–520	80–380	–323 to 1505	-100. Up to 700 in high substitution specialised cements
Animal biomass ash ³⁸			56–376	—	145–724	
Biomass average			186 ± 126	—	461 ± 260	
Red mud	5400	(1080)	47 ± 8	7–53	128 ± 18 < 440 with acid neutralising capacity of liquor	—

Input data are presented in Supplementary Table 2 and Supplementary Note 1, all units in kg CO₂ t⁻¹

^aCalculated by dividing the emissions of the production process by the mass of alkaline material

^bPredicted future emission normalised to mass of alkaline material

^cMaximum CO₂ capture potential by forming carbonate minerals

^dCO₂ capture measured in experimental work

^eMaximum enhanced weathering CO₂ capture potential

^fCO₂ mitigation potential from other uses of material

^gSee Supplementary Notes 2 and 3

^hBased on an 80% emission reduction target²⁶ (e.g., UK and EU)

ⁱAccounting for aggregate primary energy carbon intensities in RCP2.6 by 2050. Brackets denote 2100 projected

Residue from coal and biomass combustion (e.g., fly and bottom ash) has been shown to carbonate in HTP experiments²⁷. Due to the small particle size, large surface area and the high concentration of silica, ash is readily reused as a pozzolan or binder substitution in cement production, resulting in a saving of 100–700 kg CO₂ t⁻¹ over raw material²⁸, although the extent of substitution is limited by impact on strength. Furthermore, biomass ash has a long history of being spread onto agricultural land as an alternative liming agent²⁹. Under the representative concentration pathway 2.6 (RCP2.6, the pathway most likely to result in <2 °C of warming), the emissions intensity of primary energy is predicted to decrease to 25 kg CO₂ GJ⁻¹ by 2050 and –11 kg CO₂ GJ⁻¹ by 2100³⁰; the lower negative value is a result of biomass energy carbon capture and storage. As such, carbonation or enhanced weathering of ash (up to 1800 kg CO₂ t⁻¹) from biomass power generation could represent a non-trivial additional carbon draw-down (Supplementary Note 5 and Supplementary Table 2). The elevated phosphorus or sulphur content could limit the carbonation of some biomass ashes, resulting in an emission of CO₂ through the release of acidic waters during weathering.

Aluminium is produced by digesting bauxite ore in a high temperature solution of sodium hydroxide (known as the Bayer process), the products of which are alumina and a waste residue described as red mud. Red mud is composed primarily of iron and aluminium oxide/hydroxide, carbonate or hydroxide calcium (tricalcium aluminate, hydro-calumite) or sodium (sodalite, cancrinite) aluminates³¹. The residue is typically deposited with unreacted sodium hydroxide solution or dry-stacked. Carbonation of red mud has been demonstrated in HTP and ambient reactions, although only minor uptake was measured (<50 kg CO₂ t⁻¹)^{32,33}. The maximum capacity of unsintered/causticised

red mud is 128 kg CO₂ t⁻¹. The supply of divalent cations through the addition of gypsum, calcium chloride or lime (e.g., during sintering) may further increase the carbonation of the residual solution NaOH and Na-aluminate minerals³⁴ (Supplementary Note 6).

Carbon uptake has been demonstrated in the waste materials and tailing ponds from asbestos¹⁶, nickel³⁵ and diamond³⁶ mines, and in HTP experiments³⁷. To estimate the carbon sequestration potential, we have focussed on the waste rock production from nickel and platinum group metal (PGM) mining. We have not accounted for waste from asbestos production, the future generation of which may be limited (Supplementary Note 7).

Alkaline material production forecast. By combining material economic saturation trends (see, e.g., van Ruijven et al.³⁸) with forecasts of global economic development, consumption, population and biomass/coal primary energy from shared socio-economic pathways (SSPs) and associated aggregated RCPs³⁹, it is possible to estimate future production of alkaline materials. We focus specifically on the contemporary and future production of alkaline materials, but there may also be tens of Gt of material stockpiled from historical production^{40,41}. Figure 1 shows annual per capita production/consumption of cement, steel, PGM and nickel, and lime as a function of gross domestic product (GDP) or gross world product (GWP). Nonlinear least squares regression through national and global data were used to predict future production (a list of nations is included in the Supplementary Note 8). Consumption in the SSPs has been normalised to 2005 and used to derive relative changes to the baseline.

Maximum (SSP2) 2100 production estimates for cement, steel, aluminium and lime are 7.5 ± 0.4 Gt yr⁻¹, 7.1 ± 0.1 Gt yr⁻¹,

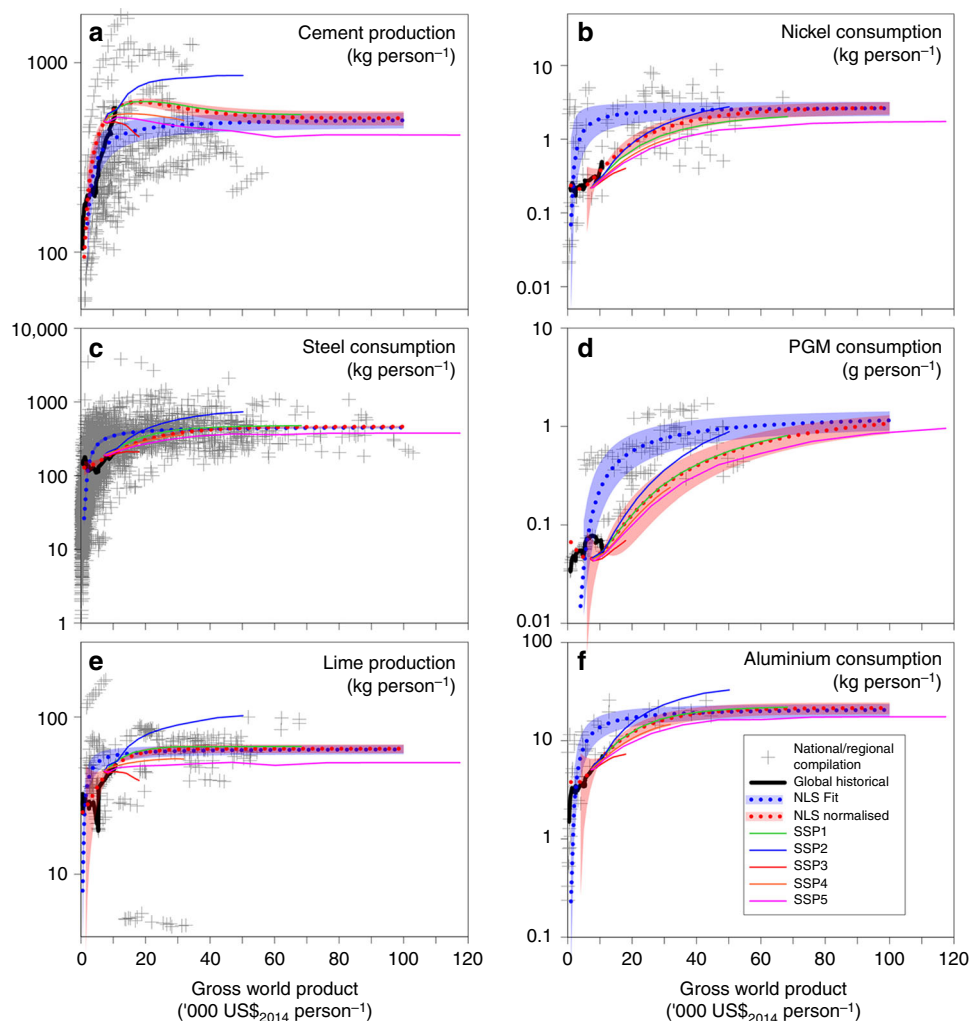


Fig. 1 Consumption/production global saturation estimates for alkaline materials. **a** Cement, **b** nickel, **c** steel, **d** platinum group metal (PGM), **e** lime and **f** aluminium as a function of gross world product (GWP). The diagrams show a nonlinear least squares regression through compiled national data (blue dotted, the shading represents \pm the standard error). The saturation value from this was fixed in an additional regression using global data relative to 2014 consumption (red dotted). Using the global fit as a baseline, the relative consumption projections for the shared socio-economic pathways (SSPs) were derived by normalising absolute changes in consumption. Production has been used for lime and cement that have a relatively small international trade market (<5%), otherwise apparent consumption has been plotted using national (slag) or regional (aluminium, PGM, nickel) data

$334 \pm 34 \text{ Mt yr}^{-1}$ and $900 \pm 35 \text{ Mt yr}^{-1}$ respectively (Fig. 2). Approximately 8–15% of the cement production is kiln dust which equates to between 245 Mt yr^{-1} and 1.1 Gt yr^{-1} by 2100. Approximately 300 Mt of concrete demolition waste are currently produced annually from a concrete stock of around 315 Gt⁴². Our model predicts production of demolition waste may increase to $20\text{--}40 \text{ Gt yr}^{-1}$ by 2100. Steel and blast furnace slag production may increase to 2.2 and 0.7 Gt yr^{-1} respectively by the end of the century. Red mud from aluminium production may increase from 150 Mt yr^{-1} currently to $500\text{--}1100 \text{ Mt yr}^{-1}$ by 2100. Primary energy from coal combustion in the SSP baseline scenarios is anticipated to vary between recent production 120 EJ yr^{-1} to $>880 \text{ EJ yr}^{-1}$. The RCP compilations largely predict decreases in coal use to $<60 \text{ EJ yr}^{-1}$ for 2.6. Assuming a coal mix that changes from current levels (10% lignite, and 90% hard coal of bituminous/antracite, with ash contents $\sim 10\%$) to zero lignite by 2100, the total ash production varies between 130 Mt yr^{-1} and 4.2 Gt yr^{-1} . An inverse relationship is predicted for biomass energy production, with ash production ranging from 300 Mt yr^{-1} (SSP5) to 1.2 Gt yr^{-1} in the RCP2.6 compilation. Up to 3.5 Gt yr^{-1} of ultrabasic mine tailings (SSP2) may be

produced by 2100 because of extracting $\sim 25 \text{ Mt yr}^{-1}$ of nickel and $\sim 5 \text{ kt yr}^{-1}$ of platinum group elements (see Supplementary Figs. 1–5 for material-specific production forecasts and associated carbonation potential).

Discussion

The results suggest that the global CO_2 carbonation potential may increase from $1 \text{ GtCO}_2 \text{ yr}^{-1}$, which is consistent with previous estimates based on current production⁴⁰, to between 2.3 and $3.3 \text{ GtCO}_2 \text{ yr}^{-1}$ in 2050 and 2.9 and $5.9 \text{ GtCO}_2 \text{ yr}^{-1}$ by 2100 (Fig. 3). Trends in material consumption (high in SSP2, status in SSP5) drive the larger difference between these scenarios, with relative changes in GDP or population between other scenarios diminishing the difference in CO_2 capture potentials. Global CO_2 emissions in the baseline SSP scenarios in 2100 range from $24 \text{ GtCO}_2 \text{ yr}^{-1}$ (SSP1) to $126 \text{ GtCO}_2 \text{ yr}^{-1}$ (SSP5). Carbonating alkaline waste materials may mitigate between 5 and 12% of these baseline emissions. The lower emission RCPs predict CO_2 emissions to reach zero later this century and become net negative by up to $16 \text{ GtCO}_2 \text{ yr}^{-1}$ (RCP2.6) in 2100³. As such,

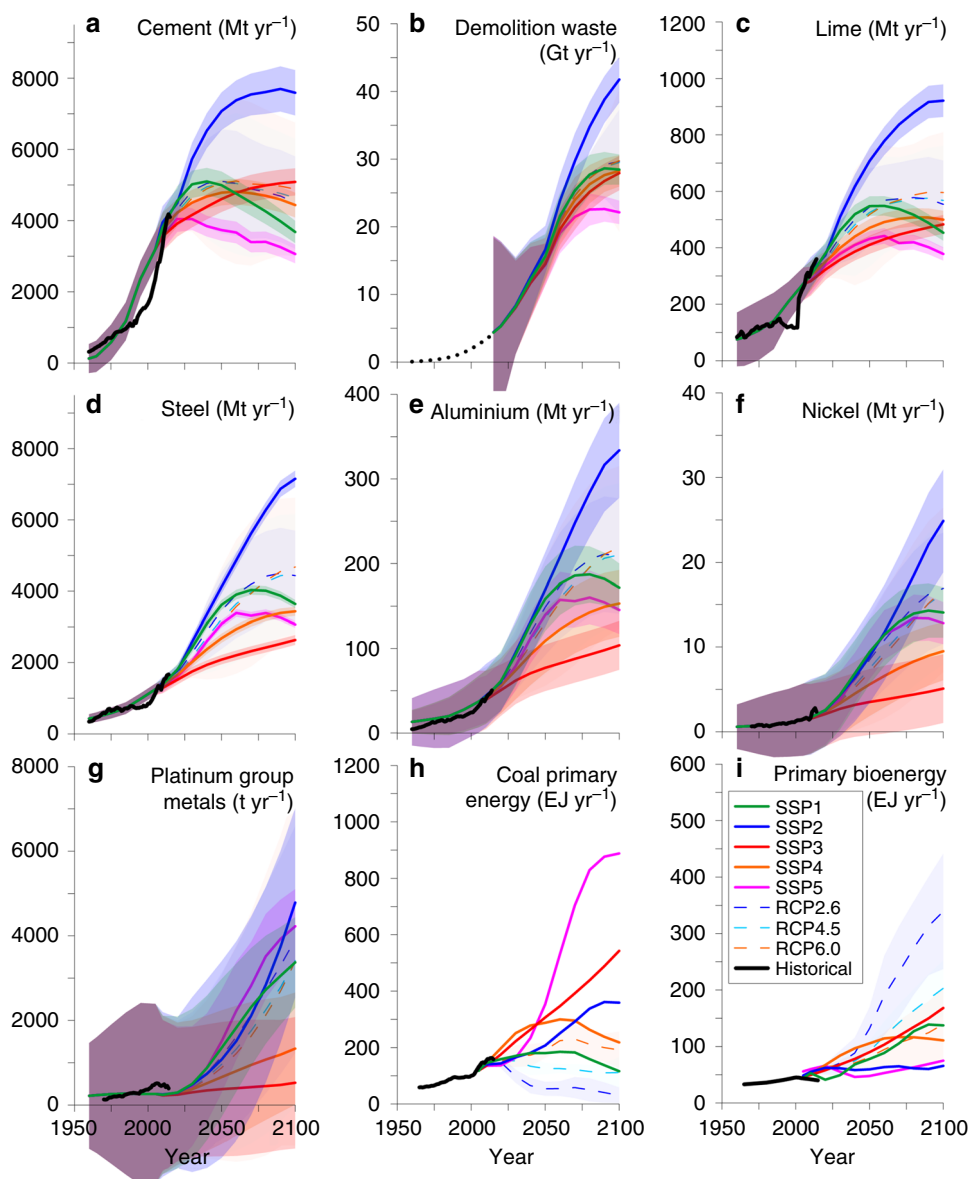


Fig. 2 Production estimates for alkaline materials. **a** Cement, **b** demolition waste, **c** lime, **d** steel, **e** aluminium, **f** nickel, **g** platinum group metals, **h** coal primary energy and **i** primary bioenergy. Historical material production⁵⁸ and energy use⁴⁹ are also shown. Production forecasts were generated by combining a gross world product-per capita production saturation model, with projections of future economic growth, relative consumption, population and energy production

the carbonation of alkaline materials using atmospheric CO₂ could contribute ~18 and 37% of the negative emission requirements in RCP2.6. The enhanced weathering potential of alkaline materials (see Supplementary Fig. 6) ranges between 2.6 and 3.8 GtCO₂yr⁻¹ in 2050, and increases to between 4.3 (SSP5) and 8.5 (SSP2) GtCO₂yr⁻¹ by 2100. This is comparable to estimated potentials of other methods of removing CO₂ from the atmosphere. For instance, a recent synthesis report from the National Academy of Sciences, Engineering, and Medicine² suggest safe global scalable levels of sequestration to be 1–1.5 GtCO₂yr⁻¹ for afforestation or forest management, 3 GtCO₂yr⁻¹ for soil carbon management and 3.5–5.2 GtCO₂yr⁻¹ for biomass energy carbon capture and storage. However, the land requirements of CO₂ capture using alkaline materials are considerably less.

These projections represent a theoretical maximum potential, which, in practice, would be difficult to realise. Research

investigating carbon uptake using these materials has primarily focused on HTP reactor experiments^{11–13,27,32,37}, which are typically far from optimised. Considerably more research is required to assess the potential for optimising CO₂ capture at ambient conditions.

Production data for many of these materials are typically not reported, and inventory assessments of current stockpiles are unlikely to be publicly available. As such, it is only possible to estimate production, as we have done, through proxy information. A more robust accounting mechanism is required to accurately assess the potential of alkaline materials.

Furthermore, there is no national or international mechanism for accounting for the value of CO₂ capture in waste. While this may be relatively trivial for carbonating materials emanating from a production site, it is more complicated for cement and lime where the latent carbon sequestration potential is only realised after many years of service life.

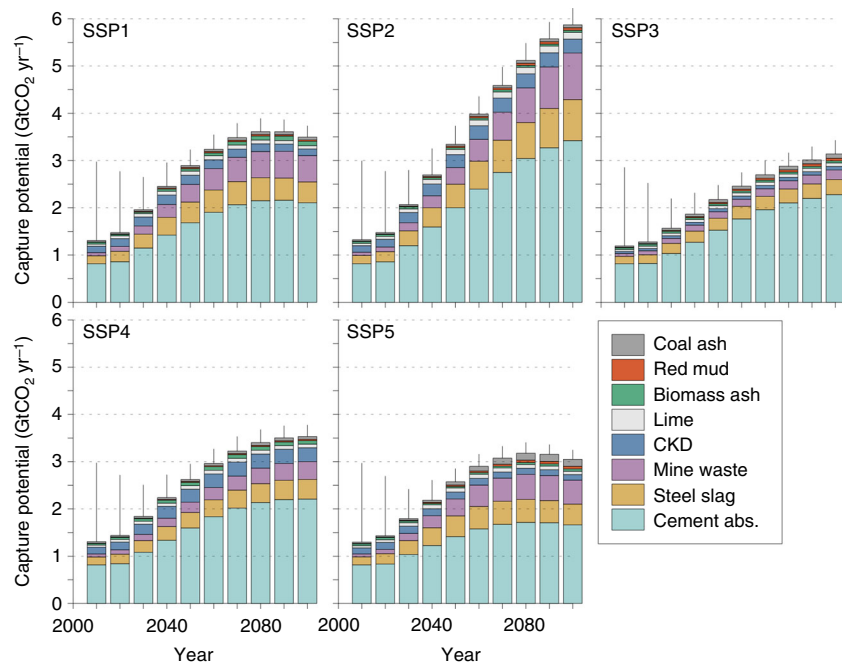


Fig. 3 Forecast of CO₂ capture potential through carbonation of alkaline materials to 2100 for the baseline shared socio-economic pathways (SSPs). The error bars represent the standard error for the range of concentration pathways in the SSPs ($n = 4$ for SSPs 1 and 3, and $n = 5$ for SSPs 2, 4 and 5) together with uncertainties of material production and consumption, and chemistry

The economic cost of capturing CO₂ using alkaline materials could be relatively low as most are available as wastes or low-value by-products, and typically in particle sizes that facilitate rapid reaction. There may be additional processing costs (particularly in supplying CO₂ or water to the reaction site), which may lower the efficiency of the proposals. These costs should be explored further and included within integrative assessment models to consider the wider carbon balances of reacting atmospheric CO₂ alkaline wastes.

Before deployment at scale it is imperative that the environmental and social consequences of these activities are explored. Carbonate formation in alkaline waste materials has long been associated with lowering their environmental burden²², whereas ash and slag have been used positively as replacement lime for agriculture. However, these materials are heterogeneous, and individual production sites will require unique and ongoing assessments.

Exploiting opportunities in existing industries for atmospheric CO₂ sequestration may contribute significantly to preventing climate change, by storing carbon permanently in either mineral carbonates or as dissolved bicarbonate in the ocean. It would be unwise to explore this potential at the expense of extensive emissions reduction. However, meeting the material demands of a growing global population will present an opportunity for low-cost atmospheric carbon dioxide sequestration that would be equally myopic to ignore.

Methods

Production forecast model. A model that relates national or regional per capita material production (for cement and lime) or consumption (for aluminium, steel, platinum group metals, and nickel) (P) to per capita GDP (national or regional data, see Supplementary Fig. 7 and Note 2)³⁸ was regressed through historical data using nonlinear least squares (Eq. (4)).

$$P = ae^{-b/\text{GDP}}, \quad (4)$$

where a and b are regression constants. The values returned for a and b for each material are included in the Supplementary Table 3 with their standard error. The derived saturation value, a , was used in a further regression through global data

normalised to 2014 production and GDP (Eq. (5)).

$$P = P_{\text{REF}} \times (1 + ((m + r) \times \Delta\text{GWP}) \times e^{(a \times (1 - e^{-(m \times \Delta\text{GWP})})) - (m \times \Delta\text{GWP})}), \quad (5)$$

where P_{REF} is the global per capita consumption at a given reference year (2014), ΔGWP is the deviation of the per capita GWP from the reference year; and m and r are regression constants, for which m was fixed and r varied (a sensitivity analysis for variations in m was performed to minimise the standard error for r). This formed the baseline which was modified with relative normalised consumption intensities (C_t/C_{2005}) for each SSP and RCP derivative. The per capita consumption model was combined with GWP capita⁻¹ and population forecasts (Pop) associated with the SSPs, to derive production forecasts (T) for cement, steel, aluminium, lime, PGM and nickel (Eqs. (6) and (7)).

$$P_{\text{norm}} = P \times \frac{C_t}{C_{2005}}. \quad (6)$$

$$T(t) = P_{\text{norm}} \times \text{Pop}(t). \quad (7)$$

Beyond the forecast change in economic consumption, we have not considered the penetration of recycling into metals production. Recycling would reduce the production of slag and remove completely the production of red mud and mine tailings. However, the proportion of material that may be recycled is limited (e.g., 69% for steel and 65% for aluminium^{43,44}), particularly for developing economies yet to reach saturation. As such, we may overestimate the contribution of CO₂ removal using slag, mine tailings or red mud. Cement, cement kiln dust, lime and ash have no capacity to be recycled as the original materials.

For every tonne of clinker, 115 ± 17 kg of cement kiln dust is produced as a by-product in kilns. While the latent capacity of CO₂ uptake in cement could be partially realised through elevated CO₂ curing (see, e.g., ref.²³), we have only modelled carbonation/weathering through reabsorption during a 50-year service life (based on the method in ref.²⁴ and carbonation/weathering following demolition; see refs.^{11,14}, Supplementary Note 3, Supplementary Tables 4 and 5). Of the lime production, 20% was assumed available for reaction with CO₂ (see Supplementary Note 4). The ratio of pig iron to steel production (0.724 ± 0.002) was found using linear regression of 1960–2014 data, negating the need to explicitly model pig iron displacement from scrap recycling, assuming the scrap ratio remains unchanged. All steel and blast furnace slags were considered available for reaction with CO₂. While a substantial proportion of blast furnace slag is recycled as aggregate or for clinker replacement¹⁸, we assume that the value (cost and carbon) is greater for reaction with atmospheric CO₂ than for clinker replacement (e.g., Table 1). If the silicon was extracted from the slag prior to carbonation, recycling and CO₂ capture may not be mutually exclusive. Between 2006 and 2014, there was 185 ± 5 kg of blast furnace slag and 117 ± 5 kg of steel slag produced for every tonne of crude steel⁴³. Between 1967 and 2014, 3.5 ± 0.04 tonnes of red mud were produced for every tonne of aluminium (see Supplementary Note 6)⁴⁵. Approximately 60% of nickel reserves are contained within ultrabasic laterite

deposits (containing $1.2 \pm 0.4\%$ s.d. Ni^{46,47}), the remaining proportion is associated with nickel sulphide deposits (containing $0.4 \pm 0.4\%$ s.d. Ni⁴⁷), the ratio of which we have assumed for future production. Approximately 81 ± 24 and 234 ± 253 tonnes of ultrabasic gangue (the non-commercial proportion of the ore) are produced for every tonne of nickel from laterite and sulfidic deposits respectively (Supplementary Note 7)⁴⁷. Approximately 84% of base reserve PGM deposits are contained in ultramafic rock (containing 4.7 ± 0.7 g Pt and Pd t⁻¹⁴⁸), which has been used in this model. The remaining reserves are contained in nickel sulphide deposits and have not been considered to avoid double counting with the above. For every kg of PGM produced, 212 ± 31 tonnes of ore are processed.

Projections of future biomass and coal primary energy generation were taken from refs.⁴⁹, and combined with average higher heating values and ash contents (see Supplementary Note 5) to estimate future production of ash (Eq. (8)).

$$T(t) = E(t) \times \text{HHV} \times A, \quad (8)$$

where E is the primary energy generation, HHV is the higher heating value and A is ash content. For all materials, the production forecast is multiplied by the carbonation or enhanced weathering potential (Table 1).

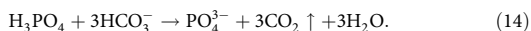
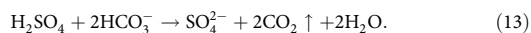
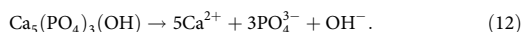
The CO₂ sequestration capacity of alkaline materials. The carbonation (C_{pot} , Eqs. (1 + 3) and Eqs. (2 + 3), expressed in kg CO₂ t⁻¹) or enhanced weathering potential (E_{pot} , Eqs. (1) and (2)) for each material (example minerals are presented in Supplementary Table 6) was derived using the bulk elemental composition of iron and steel slag⁵⁰, cement, cement kiln dust¹³, demolition waste⁴⁰, lime⁵¹, coal ash^{52,53}, biomass ash⁵⁴, red mud³¹ and PGM⁵⁵ and Ni⁵⁶ tailings in the modified Steunour formula⁵⁷ (Eqs. (9) and (10)).

$$C_{\text{pot}} = \frac{M_{\text{CO}_2}}{100} \cdot \left(\alpha \frac{\text{CaO}}{M_{\text{CaO}}} + \beta \frac{\text{MgO}}{M_{\text{MgO}}} + \gamma \frac{\text{SO}_3}{M_{\text{SO}_3}} + \delta \frac{\text{P}_2\text{O}_5}{M_{\text{P}_2\text{O}_5}} \right) \cdot 10^3, \quad (9)$$

$$E_{\text{pot}} = \frac{M_{\text{CO}_2}}{100} \cdot \left(\alpha \frac{\text{CaO}}{M_{\text{CaO}}} + \beta \frac{\text{MgO}}{M_{\text{MgO}}} + \epsilon \frac{\text{Na}_2\text{O}}{M_{\text{Na}_2\text{O}}} + \theta \frac{\text{K}_2\text{O}}{M_{\text{K}_2\text{O}}} + \gamma \frac{\text{SO}_3}{M_{\text{SO}_3}} + \delta \frac{\text{P}_2\text{O}_5}{M_{\text{P}_2\text{O}_5}} \right) \cdot 10^3 \cdot \eta, \quad (10)$$

where CaO, MgO, SO₃, P₂O₅, Na₂O and K₂O are the elemental concentrations of Ca, Mg, S, P, Na and K, expressed as oxides (Supplementary Table 7), M_x is the molecular mass of those oxides; coefficients α , β , γ , δ , ϵ , and θ consider the relative contribution of each oxide (Supplementary Figs 8 and 9); and η is molar ratio of CO₂ to divalent cation sequestered during enhanced weathering. Equations (1) and (2) imply $\eta = 2$; however, due to buffering in the carbonate system, the value is between 1.4 and 1.7 for typical seawater chemistry, pCO₂ and temperature⁸. We have used $\eta = 1.5$, which is a conservative global average. The values of carbonation and enhanced weathering potential of alkaline materials is shown in Table 1, columns c and e, respectively.

Equations (9) and (10) imply that the potential is reduced by the presence of sulphur and phosphorus within the material. These elements are either bound to cations within the material, the dissolution reactions of which have no implicit reaction with CO₂ (Eqs. (11) and (12)), or they are present as, or may become, acid compounds which would impact the carbonate system to produce CO₂ (Eqs. (13) and (14)).



Data availability

Data generated as part of this study have been made available to download as supplementary data (Supplementary Data 1–9).

Code availability

Coding data not applicable for this study.

Received: 26 October 2018 Accepted: 8 March 2019

Published online: 28 March 2019

References

- Fuss, S. et al. Betting on negative emissions. *Nat. Clim. Change* **4**, 850 (2014).
- National Academies of Sciences, Engineering, and Medicine. *Negative Emissions Technologies and Reliable Sequestration: A Research Agenda* (The National Academies Press, Washington, 2018).
- IPCC. *Global Warming of 1.5°C*. An IPCC Special Report on the impacts of global warming of 1.5°C above pre-industrial levels and related global greenhouse gas emission pathways, in the context of strengthening the global response to the threat of climate change, sustainable development, and efforts to eradicate poverty (Intergovernmental Panel on Climate Change, Incheon, 2018).
- Vaughan, N. E. et al. Evaluating the use of biomass energy with carbon capture and storage in low emission scenarios. *Environ. Res. Lett.* **13**, 044014 (2018).
- Fajardy, M. & Mac Dowell, N. Can BECCS deliver sustainable and resource efficient negative emissions? *Energy Environ. Sci.* **10**, 1389–1426 (2017).
- Minx, J. C. et al. Negative emissions—Part 1: research landscape and synthesis. *Environ. Res. Lett.* **13**, 063001 (2018).
- Renforth, P. & Henderson, G. Assessing ocean alkalinity for carbon sequestration. *Rev. Geophys.* **55**, 636–674 (2017).
- Hartmann, J. et al. Enhanced chemical weathering as a geoengineering strategy to reduce atmospheric carbon dioxide, supply nutrients, and mitigate ocean acidification. *Rev. Geophys.* **51**, 113–149 (2013).
- Lackner, K. S., Wendt, C. H., Butt, D. P., Joyce, E. L. & Sharp, D. H. Carbon dioxide disposal in carbonate minerals. *Energy* **20**, 1153–1170 (1995).
- Mayes, W. M. et al. Atmospheric CO₂ sequestration in iron and steel slag: Consett, County Durham, United Kingdom. *Environ. Sci. Technol.* **52**, 7892–7900 (2018).
- Fernández Bertos, M., Simons, S. J. R., Hills, C. D. & Carey, P. J. A review of accelerated carbonation technology in the treatment of cement-based materials and sequestration of CO₂. *J. Hazard. Mater.* **112**, 193–205 (2004).
- Huijgen, W. J. J. & Comans, R. N. J. Mineral CO₂ sequestration by steel slag carbonation. *Environ. Sci. Technol.* **39**, 9676–9682 (2005).
- Huntzinger, D. N., Gierke, J. S., Kawatra, S. K., Eisele, T. C. & Sutter, L. L. Carbon dioxide sequestration in cement kiln dust through mineral carbonation. *Environ. Sci. Technol.* **43**, 1986–1992 (2009).
- Washbourne, C.-L., Renforth, P. & Manning, D. A. C. Investigating carbonate formation in urban soils as a method for capture and storage of atmospheric carbon. *Sci. Total Environ.* **431**, 166–175 (2012).
- Renforth, P., Manning, D. A. C. & Lopez-Capel, E. Carbonate precipitation in artificial soils as a sink for atmospheric carbon dioxide. *Appl. Geochem.* **24**, 1757–1764 (2009).
- Wilson, S. A. et al. Carbon dioxide fixation within mine wastes of ultramafic-hosted ore deposits: examples from the Clinton Creek and Cassiar Chrysotile Deposits, Canada. *Econ. Geol.* **104**, 95–112 (2009).
- Vogl, V., Åhman, M. & Nilsson, L. J. Assessment of hydrogen direct reduction for fossil-free steelmaking. *J. Clean. Prod.* **203**, 736–745 (2018).
- Roy, D. M. & Idorn, G. M. Hydration, structure, and properties of blast furnace slag cements, mortars, and concrete. *J. Proc.* **79**, 444–457 (1982).
- Ahmedzade, P. & Sengoz, B. Evaluation of steel slag coarse aggregate in hot mix asphalt concrete. *J. Hazard. Mater.* **165**, 300–305 (2009).
- Davis, F., Collier, B. & Carter, O. Blast-furnace slag as agricultural liming material. *Commer. Fertil.* **80**, 48–49 (1950).
- Yi, H. et al. An overview of utilization of steel slag. *Procedia Environ. Sci.* **16**, 791–801 (2012).
- Mayes, W. M., Younger, P. L. & Aumônier, J. Hydrogeochemistry of alkaline steel slag leachates in the UK. *Water Air Soil Pollut.* **195**, 35–50 (2008).
- Young, J., Berger, R. & Brees, J. Accelerated curing of compacted calcium silicate mortars on exposure to CO₂. *J. Am. Ceram. Soc.* **57**, 394–397 (1974).
- Xi, F. et al. Substantial global carbon uptake by cement carbonation. *Nat. Geosci.* **9**, 880 (2016).
- Fleming, I. R., Rowe, R. K. & Cullimore, D. R. Field observations of clogging in a landfill leachate collection system. *Can. Geotech. J.* **36**, 685–707 (1999).
- EuLA. *A Competitive and Efficient Lime Industry*. Prepared by Ecofys (European Lime Association, 2014). <https://www.eu-la.eu/documents/competitive-and-efficient-lime-industry-cornerstone-sustainable-europe-lime-roadmap-1>.
- Montes-Hernandez, G., Pérez-López, R., Renard, F., Nieto, J. M. & Charlet, L. Mineral sequestration of CO₂ by aqueous carbonation of coal combustion fly-ash. *J. Hazard. Mater.* **161**, 1347–1354 (2009).
- Miller, S. A., Horvath, A., Monteiro, P. J. M. & Ostertag, C. P. Greenhouse gas emissions from concrete can be reduced by using mix proportions, geometric aspects, and age as design factors. *Environ. Res. Lett.* **10**, 114017 (2015).
- James, A. K., Thring, R. W., Helle, S. & Ghuman, H. S. Ash management review—applications of biomass bottom ash. *Energies* **5**, 3856–3873 (2012).
- van Vuuren, D. P. et al. The representative concentration pathways: an overview. *Clim. Change* **109**, 5 (2011).
- Gräfe, M., Power, G. & Klauber, C. Bauxite residue issues: III. Alkalinity and associated chemistry. *Hydrometallurgy* **108**, 60–79 (2011).
- Yadav, V. S. et al. Sequestration of carbon dioxide (CO₂) using red mud. *J. Hazard. Mater.* **176**, 1044–1050 (2010).
- Bonenfant, D. et al. CO₂ sequestration by aqueous red mud carbonation at ambient pressure and temperature. *Ind. Eng. Chem. Res.* **47**, 7617–7622 (2008).

34. Renforth, P. et al. Contaminant mobility and carbon sequestration downstream of the Ajka (Hungary) red mud spill: the effects of gypsum dosing. *Spec. Sect. Rev. Trace Met. Pollut. China* **421–422**, 253–259 (2012).
35. Pronost, J. et al. Carbon sequestration kinetic and storage capacity of ultramafic mining waste. *Environ. Sci. Technol.* **45**, 9413–9420 (2011).
36. Wilson, S. A., Raudsepp, M. & Dipple, G. M. Quantifying carbon fixation in trace minerals from processed kimberlite: a comparative study of quantitative methods using X-ray powder diffraction data with applications to the Diavik Diamond Mine, Northwest Territories, Canada. *Appl. Geochem.* **24**, 2312–2331 (2009).
37. Bobicki, E. R., Liu, Q., Xu, Z. & Zeng, H. Carbon capture and storage using alkaline industrial wastes. *Prog. Energy Combust. Sci.* **38**, 302–320 (2012).
38. van Ruijven, B. J. et al. Long-term model-based projections of energy use and CO₂ emissions from the global steel and cement industries. *Resour. Conserv. Recycl.* **112**, 15–36 (2016).
39. Riahi, K. et al. The shared socioeconomic pathways and their energy, land use, and greenhouse gas emissions implications: an overview. *Glob. Environ. Change* **42**, 153–168 (2017).
40. Renforth, P., Washbourne, C.-L., Taylder, J. & Manning, D. A. C. Silicate production and availability for mineral carbonation. *Environ. Sci. Technol.* **45**, 2035–2041 (2011).
41. Picot, J. C., Cassard, D., Maldan, F., Greffié, C. & Bodéan, F. Worldwide potential for ex-situ mineral carbonation. *Energy Procedia* **4**, 2971–2977 (2011).
42. Krausmann, F. et al. Global socioeconomic material stocks rise 23-fold over the 20th century and require half of annual resource use. *Proc. Natl. Acad. Sci. USA* **114**, 1880 (2017).
43. Oss, H. G. v. *Slag – Iron and Steel Mineral Commodity Summaries* (U.S. Department of the Interior and U.S. Geological Survey, 2016). https://minerals.usgs.gov/minerals/pubs/commodity/iron_&_steel_slag/.
44. Gutowski, T. G., Sahni, S., Allwood, J. M., Ashby, M. F. & Worrell, E. The energy required to produce materials: constraints on energy-intensity improvements, parameters of demand. *Philos. Trans. R. Soc. Math. Phys. Eng. Sci.* **371**, 20120003 (2013).
45. Bertram, M. et al. A regionally-linked, dynamic material flow modelling tool for rolled, extruded and cast aluminium products. *Resour. Conserv. Recycl.* **125**, 48–69 (2017).
46. Berger, V. I., Singer, D. A., Bliss, J. D. & Moring, B. C. *Ni-Co Laterite Deposits of the World: Database and Grade and Tonnage Models* (US Department of the Interior, Geological Survey, 2011). <https://pubs.usgs.gov/of/2011/1058/>.
47. Mudd, G. M. & Jowitt, S. M. A detailed assessment of global nickel resource trends and endowments. *Econ. Geol.* **109**, 1813–1841 (2014).
48. Wilburn, D. R. & Bleiwas, D. I. Platinum-group metals—world supply and demand. *US Geol. Surv. Open File Rep.* **1224**, 2004–1224 (2004).
49. Smil, V. *Energy Transitions: Global and National Perspectives* (ABC-CLIO, Santa Barbara, 2016).
50. Proctor, D. M. et al. Physical and chemical characteristics of blast furnace, basic oxygen furnace, and electric arc furnace steel industry slags. *Environ. Sci. Technol.* **34**, 1576–1582 (2000).
51. Oates, T. Lime and limestone. in *Kirk-Othmer Encyclopedia of Chemical Technology* (ed. Kirk-Othmer) 1–53 (American Cancer Society, New York, NY, 2002). <https://doi.org/10.1002/0471238961.1209130507212019.a01.pub2>.
52. Selvig, W. A. & Gibson, F. H. *Analyses of Ash from Coals of the United States* (U.S. G.P.O., Washington, 1945).
53. Dai, S. et al. Geochemistry of trace elements in Chinese coals: a review of abundances, genetic types, impacts on human health, and industrial utilization. *Miner. Trace Elem. Coal* **94**, 3–21 (2012).
54. Vassilev, S. V., Baxter, D., Andersen, L. K. & Vassileva, C. G. An overview of the composition and application of biomass ash. Part 1. Phase–mineral and chemical composition and classification. *Fuel* **105**, 40–76 (2013).
55. Vogeli, J., Reid, D. L., Becker, M., Broadhurst, J. & Franzidis, J.-P. Investigation of the potential for mineral carbonation of PGM tailings in South Africa. *Miner. Eng.* **24**, 1348–1356 (2011).
56. Marsh, E., Anderson, E., & Gray, F. Nickel–cobalt laterites—a deposit model. Chapter H of *Mineral Deposit Models for Resource Assessment*: U.S. Geological Survey Scientific Investigations Report 2010–5070–H (2013). <https://pubs.er.usgs.gov/publication/sir20105070H>.
57. Gunning, P. J., Hills, C. D. & Carey, P. J. Accelerated carbonation treatment of industrial wastes. *Waste Manag.* **30**, 1081–1090 (2010).
58. USGS. *USGS Minerals Yearbook* (U.S. Department of the Interior and U.S. Geological Survey, Reston, VA, United States, 2016).

Acknowledgements

P.R. is funded by the UK's Greenhouse Gas Removal Programme, supported by the Natural Environment Research Council, the Engineering and Physical Sciences Research Council, the Economic & Social Research Council and the Department for Business, Energy & Industrial Strategy under grant no. NE/P019943/1.

Author contributions

P.R. designed the study, undertook the calculations and wrote the manuscript.

Additional information


Supplementary Information accompanies this paper at <https://doi.org/10.1038/s41467-019-09475-5>.

Competing interests: The author declares no competing interests.

Reprints and permission information is available online at <http://npg.nature.com/reprintsandpermissions/>

Journal peer review information: *Nature Communications* thanks Georgios N. Kalantzopoulos, Gregory M. Dipple and the other anonymous reviewer for their contribution to the peer review of this work. Peer reviewer reports are available.

Publisher's note: Springer Nature remains neutral with regard to jurisdictional claims in published maps and institutional affiliations.

 **Open Access** This article is licensed under a Creative Commons Attribution 4.0 International License, which permits use, sharing, adaptation, distribution and reproduction in any medium or format, as long as you give appropriate credit to the original author(s) and the source, provide a link to the Creative Commons license, and indicate if changes were made. The images or other third party material in this article are included in the article's Creative Commons license, unless indicated otherwise in a credit line to the material. If material is not included in the article's Creative Commons license and your intended use is not permitted by statutory regulation or exceeds the permitted use, you will need to obtain permission directly from the copyright holder. To view a copy of this license, visit <http://creativecommons.org/licenses/by/4.0/>.

© The Author(s) 2019